Optimization of Electrical Properties in TiO2/WSix-based Vertical DG-MOSFET using Taguchi-based GRA with ANN

K.E.Kaharudin, F.Salehuddin, A.S.M.Zain
Centre for Telecommunication Research and Innovation, Faculty of Electronics and Computer Engineering, Universiti Teknikal Malaysia Melaka (UTeM), Hang Tuah Jaya, Durian Tunggal, 76100 Melaka
khairilezwan@yahoo.com.my

***Abstract*—This study describes a proposed method to determine the most optimal level of process parameters, considering multiple electrical properties of titanium dioxide/tungsten silicide (TiO_2/WSi_x)-based vertical double-gate MOSFET. The proposed method utilizes a combination of the L_9 orthogonal array (OA) of Taguchi-based grey relational analysis (GRA) and the artificial neural network (ANN). The V_{TH} implant energy, halo implant dose, source/drain (S/D) implant dose and S/D implant tilt angle are the selected processs parameters to be optimized for the optimal value of on-current (I_{ON}), off-current (I_{OFF}) and subthreshold slope (SS). The design of experiment (DoE) is based on the L_9 OA of Taguchi method and the experimental value for multiple electrical properties are converted into a grey relational grade (GRG). The well-trained ANN based on the Levenberg-Marquardt algorithm is developed to predict the best optimization results. The most optimal level of four process parameters towards I_{ON}, I_{OFF} and SS are selected based on the highest GRG predicted by well-trained ANN. The most optimal value for I_{ON}, I_{OFF} and SS after the optimization are observed to be 1612.1 µA/µm, 8.801E-10 A/µm and 67.74 mV/dec respectively with 0.7417 of predicted GRG.**

***Index Terms*—ANN, GRG, off-current, on-current**

I. INTRODUCTION

Ion implantation has been the dominating doping technique for silicon-based Metal-oxide-semiconductor Field Effect Transistor (MOSFET). It is still expected that ion implantation will remain as the main doping technique for future MOSFET technology. Ion implantation is a process where dopant is introduced to the silicon substrate using chemical materials such as boron, arsenic, indium and etc [1]. These materials are ionized and accelerated to a large amount of energy to form a perfect silicon surface. The implantation energies vary between 1.0kev to 1.0Mev, depending on the device's dimension [2]. For threshold voltage adjustment, the implant concentration vary from 1012 atom/cm-3 to 1018 atom/cm-3 [3]. Other types of ion implantation are known as halo implantation and source/drain (S/D) implantation.

Ion implantation consists of parameters such as the amount of dopant dosage, energy level and also the implant tilt angle which are required to be considered in MOSFET fabrication. The variations of these parameters are very crucial in order to control the the doping profile of MOSFETs [4]. There may be a reason to use a high or a low angle implant to introduce dopant underneath the gate of the MOSFET. For the purpose of the short channel effect (SCE) mitigation, doping so called 'halo' is developed by high tilt angle under the edge of the gate [5]. In most cases, the variations due to ion implantation process may influence the electrical properties of the MOSFETs [6], [7]. Therefore, special techniques involving planned and analytical experiments are required to identify the parameters that contribute the most of these variations.

Ramakrishnan in his technical report proposed a statistical method based on response surface methodology (RSM) to study the impact of process parameter fluctuations on electrical properties of 65nm MOSFET technology [8]. The results showed that ion implantation process are ranked among the top contributors of varying the electrical properties of MOSFETs. However, the implementation of RSM requires a lot of experiment runs and data in order to get the best results. An alternative solution besides RSM is known as Taguchi method which requires less experiment runs due to its special orthogonal array (OA) [9]. Salehuddin et al. in their reports employed Taguchi method to optimize multiple process parameters of 45nm MOSFETs to obtain the best electrical properties in accordance with the prediction of International Technology Roadmap (ITRS) [10], [11]. On top of that, Afifah Maheran et al. also utilized Taguchi method to tune threshold voltage (VTH) and off-current (IOFF) in 22nm gate length high-k/metal-gate MOSFETs [12], [13].

Although, Taguchi method offers less experiment runs and more simple approach, it is however restricted to a single electrical property where it is only capable of optimizing one electrical property at a time. Hence, the grey relational analysis (GRA) is combined with Taguchi method to solve multiple objective problems where multiple electrical properties can be optimized simultaneously [14]. A lot of previous reports have employed the Taguchi-based GRA approach to solve multiple objective problems in many engineering fields [15]–[17]. Another limitation of Taguchi method is that it can only find optimal solutions within the specified level of process parameters. Once the optimal level of process parameters are identified, the feasible solution space is constrained. Taguchi method is only capable of addressing discrete process parameters, not continuous process parameters [18]. Therefore artificial neural network (ANN) is introduced to Taguchi-based GRA, becoming a robust optimizer in finding the best solutions.

ANN is a non linear function, accurately representing a complex relationship between inputs and outputs [19], [20]. A trained ANN model has also been utilized to predict the output for specified input. Lin (2012) [18] described an application of ANN to optimize the weld bead geometry in a novel gas metal arc welding process. The results showed that

the well-trained ANN did enhance the efficiency of optimization approach in determining the best welding process parameter with consideration of multiple performance characteristics. Kenghe & Patare (2015) [21] utilized a combination of GRA and ANN to predict and analyze the effectiveness of parameters of specific wear rate of bearing materials. The results proved that the back propagation ANN do enhance the GRA performance to simultaneously optimize the wear and friction characteristics of bearing material. Yadav et al. (2015) [22] provided the details implementation of ANN fitting tool for prediction of solar radiations data from 14 cities of Himachal Pradesh India. The latitude, longitude, atmospheric preassure were selected as inputs while the wind speed and solar radiations were selected as outputs. The results showed that the correlation value (R) is 95.80%, implying good agreement between measured values and predicted ANN values.

This paper presents a method that combines L9 OA of Taguchi method, GRA and ANN to model and optimize the on-current (ION), off-current (IOFF) and subthreshold slope (SS) simultaneously in the TiO2/WSix-based vertical double-gate (DG) MOSFET. The proposed method consists of two stages. First stage is the initial optimization using L9 OA of Taguchi-based GRA. The second stage is the utilization of an ANN with Levenberg-Marquardt back-propagation (LMBP) algorithm to develop a well-trained ANN model, thus predicting the most optimal process parameters. The work-flow of the proposed method, combining L9 OA of Taguchi method, GRA and ANN is depicted Figure 1. The ANN application of MATLAB toolbox was used to develop the well-trained ANN model for robust optimization.

II. Device Simulation

A. *TiO2/WSix-based Vertical Double-gate MOSFET Design*

A 2-D simulation for 10nm gate length (L_g) TiO_2/WSi_x-based vertical double-gate n-channel MOSFET was performed using ATHENA module of Silvaco TCAD tools. The geometric design was contructed based on the previous report in [23], [24]. Table 1 shows the physical parameters used in the simulated device. The 2-D cross-section of the device which define the physical parameters like gate length (L_g), channel length (L_c), silicon pillar's height (H_{sp}) and etc. are illustrated in Figure 2.

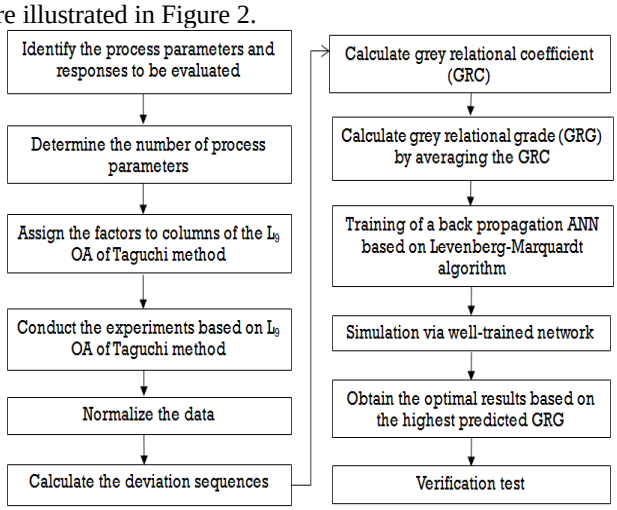

Figure 1: Work-flow of the Experimental Procedure

Table 1
Physical Parameters used in the Simulated TiO2/WSix-based Vertical Double-gate MOSFET

Parameters	Value
Gate Length (L_g)	10 nm
Gate Thickness (T_g)	9 nm
Silicon Pillar Height (H_{sp})	14 nm
Silicon Pillar Thickness (T_{sp})	15 nm
TiO_2 Thickness	3 nm
Spacer Nitride Thickness (T_{Si3Ni4})	15 nm
Channel Length (L_c)	20 nm
Metal-gate Workfunction (WF)	4.5 eV

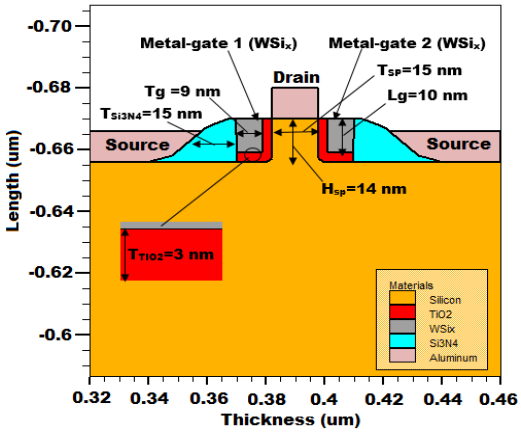

Figure 2: Cross section of 10nm Lg of $WSix/TiO_2$-based Vertical Double-gate NMOS

B. *Device Simulation*

The device simulation of the 10nm gate length TiO_2/WSi_x-based vertical double-gate MOSFET was executed using an ATLAS module of Silvaco TCAD tools. Figure 3 depicts the contour mode of the device, visualizing the tabulation of silicon, WSi_x, TiO_2, silicon nitride (Si_3Ni_4) and aluminum. Figure 4 shows the subthreshold I_D vs. V_G curve at V_D = 0.05 V and V_D = 1.0 V for the device. The initial value of I_{ON}, I_{OFF} and SS were observed to be 1588.3 µA/µm, 8.477E-10 A/µm and 68.24 mV/dec respectively. The switching speed of the device is determined by the subthreshold slope (SS) which indicates how much gate voltage required to increase one decade of drain current (I_D). The steeper the slope is, the faster the device will be. The SS characteristic was extracted from the inverse slope of $\log_{10} I_D$ vs V_{GS} characteristic shown in (1) [25]:

$$SS = \left[\frac{d(\log_{10} I_{DS})}{dV_{GS}} \right]^{-1} \quad (1)$$

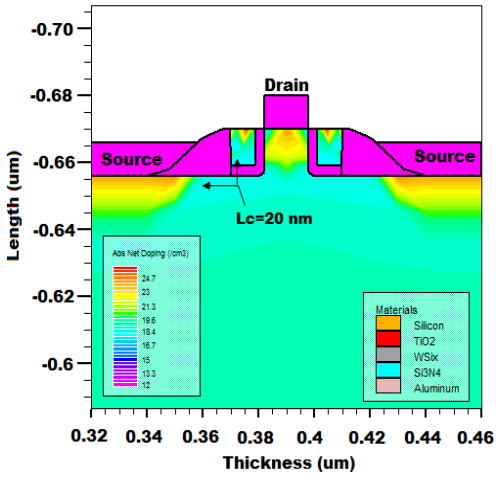

Figure 3: Contour Mode of 10nm Lg of WSix/TiO_2-based Vertical Double-gate NMOS

III. Simultaneous Optimization Of I_{ON}, I_{OFF} And SS

In this study, the L_9 OA of Taguchi method was combined with a grey relational analysis (GRA) in order to optimize multiple electrical characteristics of the device. The L_9 OA was selected for this study because it only deals with only four input process parameters. Furthermore, the L_9 OA offers a simplified design of experiment (DoE), involving a minimum number of nine experiments, which significantly reduces time and cost. The steps for conducting a simultaneous optimization by using L_9 OA of Taguchi-based GRA approach is shown in Figure 4.

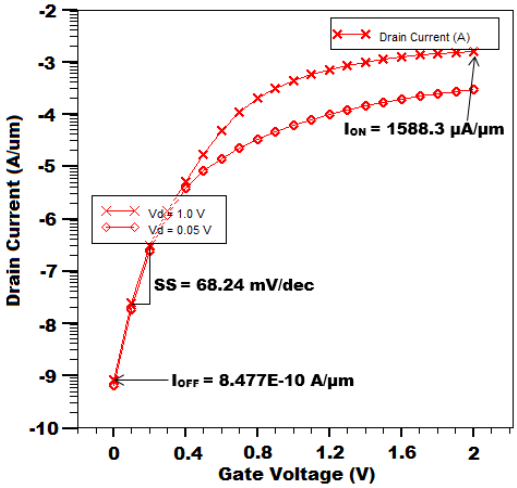

Figure 4: Graph of subthreshold drain current (I_D)-gate voltage (V_G)

A. L_9 Orthogonal Array (OA) of Taguchi Method

There are four process parameters selected in this study, which are V_{TH} implant energy, halo implant dose, S/D implant dose and S/D implant tilt angle. These process parameters are the significant factors that contributes to the variation of I_{ON}, I_{OFF} and SS [26], [27]. Since this study involved four process parameters, the L_9 OA of Taguchi method was utilized to construct a design of experiment (DoE). Table 2 shows the detailed process parameters and their levels. Table 3 shows the multiple levels of process parameters with their corresponding electrical properties. The information in Table 3 was utilized to investigate the effects of process parameters on I_{ON}, I_{OFF} and SS values.

Table 2
Process Parameters of TiO2/WSix-based Vertical Double-gate NMOS

Sym.	Process Parameter	Units	Level 1	Level 2	Level 3
A	V_{TH} Implant Energy	kev	20	22	24
B	Halo Implant Dose	atom/cm^{-3}	2.87E13	2.89E13	2.91E13
C	S/D Implant Dose	atom/cm^{-3}	2.21E18	2.23E18	2.25E18
D	S/D Implant Tilt Angle	degree	76	77	78

Table 3
L_9 Orthogonal Array Table for Responses

Exp no.	Parameter Level A	B	C	D	I_{ON} (V)	I_{OFF} (10^{-10}) (A/µm)	SS (mV/dec)
1	1	1	1	1	1588.3	8.477	68.24
2	1	2	2	2	1577.4	8.354	68.45
3	1	3	3	3	1567.5	8.203	68.67
4	2	1	2	3	1581.6	8.446	68.37
5	2	2	3	1	1589.3	8.483	68.21
6	2	3	1	2	1576.9	8.351	68.46
7	3	1	3	2	1592.8	8.610	68.14
8	3	2	1	3	1581.3	8.447	68.37
9	3	3	2	1	1589	8.484	68.23

B. Data Normalization

Multiple electrical properties of the device were investigated using GRA. GRA approach allows multiple electrical properties like I_{ON}, I_{OFF} and SS, being converted into a single grey relational grade (GRG). Initially, all the electrical properties retrieved from L_9 OA of Taguchi method were normalized in the range of 0 to 1. These electrical characteristics are categorized into different performance characteristics where I_{ON} was classified into higher-the-better performance characteristics, while I_{OFF} and SS were classified into lower-the-better performance characteristics. The following equations were used to normalize the electrical characteristics, respectively [28]:

$$x_i^*(k) = \frac{x_i(k) - \min x_i(k)}{\max x_i(k) - \min x_i(k)}, \text{ higher-the-better} \quad (2)$$

$$x_i^*(k) = \frac{\max x_i(k) - x_i(k)}{\max x_i(k) - \min x_i(k)}, \text{ lower-the-better} \quad (3)$$

where $x_i^*(k)$ and $x_i(k)$ are the sequence after data pre-processing and comparability sequence. Table 4 shows the normalized sequence of all the responses based on their corresponding performance characteristics.

Table 4
Normalized Response Values for Conducted Experiments

Exp. no	I_{ON}	I_{OFF}	SS
Reference Sequence	1	1	1
1	0.8221	0.3268	0.8113
2	0.3913	0.6290	0.4151
3	0	1	0
4	0.5573	0.4029	0.5660
5	0.8617	0.3120	0.8679
6	0.3715	0.6364	0.3962
7	1	0	1
8	0.5455	0.4005	0.5660
9	0.8498	0.3096	0.8302

C. Derivation Sequences

$\Delta_{oi}(k)$ is the deviation sequence of the reference sequence $x_o^*(k)$ and the comparability sequence $x_i^*(k)$ as shown in (4) [28]:

$$\Delta_{oi}(k) = | x_o^*(k) - x_i^*(k) | \quad (4)$$

The deviation sequences were calculated and summarized in Table 5.

Table 5
Deviation Sequences

Deviation sequences	Δ_{0i} (1)	Δ_{0i} (2)	Δ_{0i} (3)
Exp no. 1	0.1779	0.6732	0.1887
Exp no. 2	0.6087	0.3710	0.5849
Exp no. 3	1	0	1
Exp no. 4	0.4427	0.5971	0.4340
Exp no. 5	0.1383	0.6880	0.1321
Exp no. 6	0.6285	0.3636	0.6038
Exp no. 7	0	1	0
Exp no. 8	0.4545	0.5995	0.4340
Exp no. 9	0.1502	0.6904	0.1698

D. Grey Relational Coefficient and Grade

After data normalization is done, a grey relational coefficient (GRC) is computed with the pre-processed sequence. The GRC is defined as follows [28]:

$$\xi_i(k) = \frac{\Delta_{\min} + \xi\Delta_{\max}}{\Delta_{oi}(k) + \xi\Delta_{\max}} \quad (5)$$

where ξ is a n identification coefficient. Since all the process parameters are given and equal preference, ξ is taken as 0.5, while Δ_{max} and Δ_{min} are the maximum and minimum absolute difference. The GRG for each experiments was calculated by averaging the GRCs for I_{ON}, I_{OFF} and SS. The rank of each experiment was tabulated based on the highest GRG as listed in Table 6. The higher level of GRG implies the quality of multi-response characteristics.

Table 6
GRC with GRG and Their Rank

Exp. no.	GRC			GRG	Rank
	I_{ON} ξ_i(1)	I_{OFF} ξ_i(2)	SS ξ_i(3)		
1	0.7376	0.4262	0.7260	0.6299	4
2	0.4510	0.5741	0.4609	0.4953	8
3	0.3333	1	0.3333	0.5555	5
4	0.5304	0.4557	0.5353	0.5071	6
5	0.7833	0.4209	0.7910	0.6651	2
6	0.4431	0.5790	0.4530	0.4917	9
7	1	0.3333	1	0.7778	1
8	0.5238	0.4548	0.5353	0.5046	7
9	0.7690	0.4200	0.7465	0.6452	3

E. GRG for Process Parameter Levels.

Based on Table 6, experiment row no. 7 has the best multiple performance properties due to its highest GRG. Since the design of experiments is orthogonal, the GRG at different levels can be separate out. For example, the mean of the GRG for factor A (V_{TH} implant energy) at level 1 can be computed by averaging the GRG at the experiment row 1 to 3 as level 1 was allocated for column factor A as shown in Table 3. All the computed GRG for all the process parameters are listed in Table 7.

Table 7
Average GRG by Process Parameter Levels

Sym.	Process Parameters	Grey Relational Grade		
		Level 1	Level 2	Level 3
A	V_{TH} Implant Energy	0.5602	0.5546	0.6425
B	Halo Implant Dose	0.6383	0.5550	0.5641
C	S/D Implant Dose	0.5421	0.5492	0.6661
D	S/D Implant Tilt Angle	0.6467	0.5883	0.5224

The GRGs for each process parameters were then converted into factor effect graph to clearly distinguish the optimal value for each of the process parameters as shown in Figure 4. Basically, the higher GRG indicates the better the overall quality of the electrical properties. Figure 5 shows the most optimal value of process parameters based on the highest GRG which are $A_3B_1C_3D1$. The predicted GRG of the optimal level of process parameters for the device can be computed by using (7):

$$\hat{\gamma} = \gamma_m + \sum_{i=1}^{q} (\gamma_i - \gamma_m) \quad (6)$$

where is the total means of GRG , $\hat{\gamma}$ is the mean of GRG at optimal level and q is the number of process parameters. The predicted GRG is calculated as follows:

$$\hat{\gamma} = 0.5858 + (0.6425 - 0.5858) + (0.6383 - 0.5858) + (0.6661 - 0.5858) + (0.6467 - 0.5858)$$

$$\hat{\gamma} = 0.8362$$

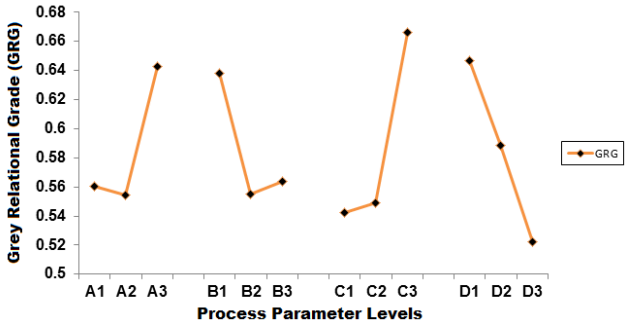

Figure 5: Factor effect plot of GRGs for Multiple Responses

IV. Optimization using Artificial Neural Network

Artificial neural network (ANN) is utilized to model complex manufacturing processes, typically process and quality control. The Levenberg-Marquardt back propagation (LMBP) algorithm is selected to model a well-trained ANN due to its faster training time. An ANN with the LMBP algorithm is used to provide the non-linear relationship between process parameters and GRG. The LMBP algorithm is the fastest algorithm for training multi-layer networks, despite of having a matrix inversion at each iteration. The development of a well-trained ANN was conducted using MATLAB application tools. Figure. 6 shows the interface between device simulator, Taguchi-based GRA and ANN. The device are simulated based on four variables. Then, the multiple characteristics, I_{ON}, I_{OFF}, SS are converted into nine GRGs. The combination of the process parameters based on nine experiments and the nine GRGs are fed into neural network to be trained. Based on the training, nine predicted

GRGs are produced. The well trained network will be the medium to tune the best process parameter that will result in the most optimum value for I_{ON}, I_{OFF} and SS.

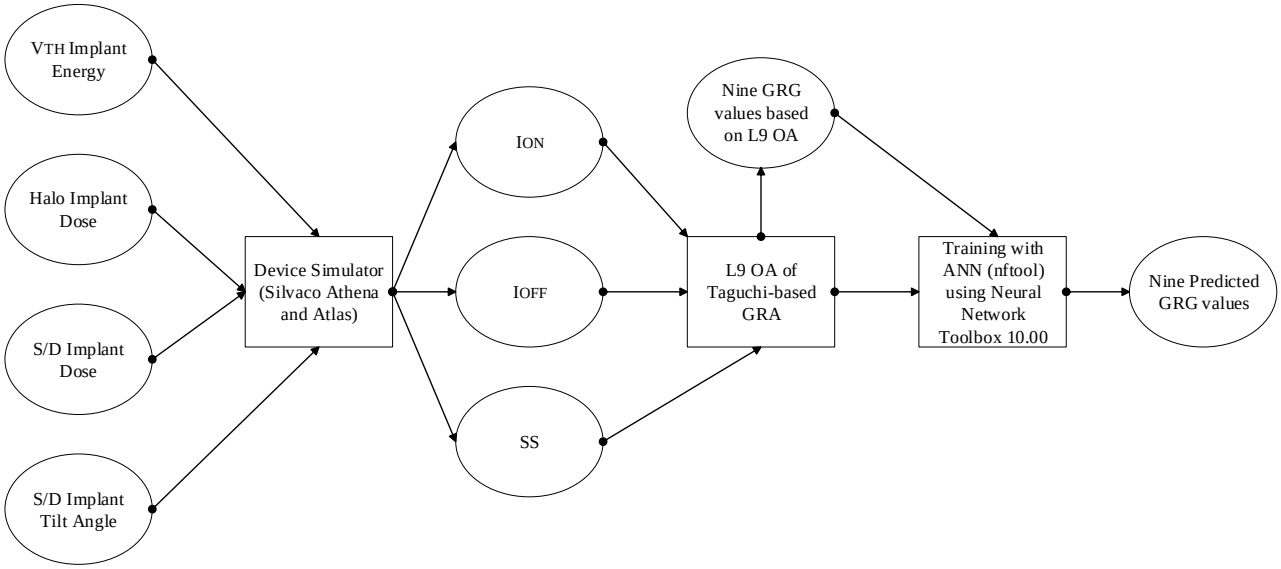

Figure 6: The interface between device simulator, Taguchi-based GRA and ANN

A. Training of Back Propagation Network

A feed forward back propagation network is typically consists of an input layer, one or more hidden layers and one output layer. For this study, it takes set of four input values which are V_{TH} implant energy, halo implant dose, S/D implant dose and S/D implant tilt angle and predicts one output value which is GRG. The transfer functions for all hidden neurons are set to be tangent sigmoid functions while the output neurons are set as a linear function. Figure 7 shows the topology of the network. Prediction outputs for ANN based on LMBP algorithm are shown in Table 8. The linear regression between network output and corresponding target is depicted in Figure 8.

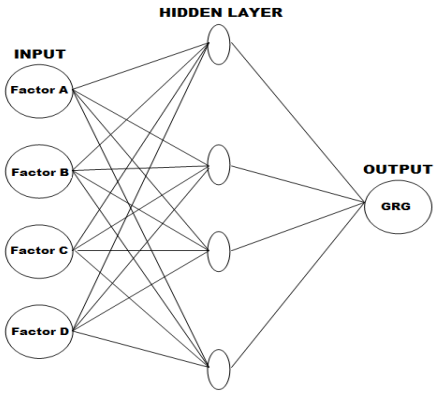

Figure 7: The LMBP Network Topology

Table 8
Predicted GRGs via well-trained ANN

Exp. no.	Actual GRG	Predicted GRG via Trained Network	Net Error	Rank
1	0.6299	0.6219	0.0008	4
2	0.4953	0.5081	0.0128	7
3	0.5555	0.5048	0.0507	9
4	0.5071	0.5263	0.0192	5
5	0.6651	0.6598	0.0053	2
6	0.4917	0.5070	0.0153	8
7	0.7778	0.7267	0.0511	1
8	0.5046	0.5185	0.0139	6
9	0.6452	0.6283	0.0169	3

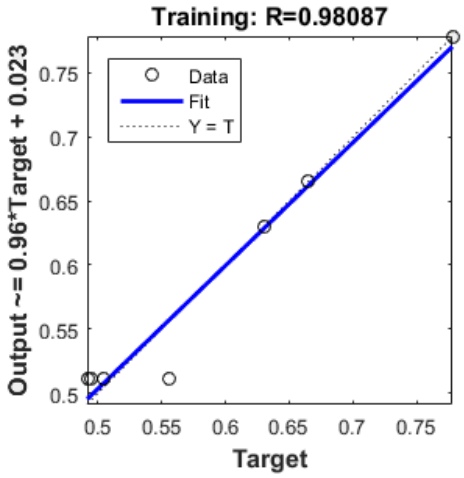

Figure 8: Regression Plot for LMBP Algorithm

Based on the training results from Table 8, the predicted GRGs are very close and follow almost the similar trend as the actual GRGs with minimum percentage error. Figure 7 indicates the dashed in each plot, representing the perfect results – outputs = targets while the solid line represents the best fit linear regression line between outputs and targets. The R value is an indication of the relationship between the outputs and targets. If R = 1, this indicates that there is an exact linear relationship between outputs and targets. If R is close to zero, then there is no linear relationship between outputs and targets. In this case, the training data indicate a good fit where R value is greater than 0.9.

B. Simulation via a well-trained ANN

The best level of process parameters predicted via L_9 OA of Taguchi-based GRA ($A_3B_1C_3D_1$) were simulated using a well-trained ANN. The predicted output (GRG) after the

simulation was observed to be 0.7393. There was a slight net error for approximately 11.6% compared to the actual GRG (0.8362). In order to enhance the performance of the optimization process, the simulation via well-trained ANN was employed where one process parameter was varied into multiple level whereas the others remained constant at the predicted optimal level.

The factor A (V_{TH} implant energy) level was varied from 24kev to 28kev, while the others were kept constant at the predicted optimal level ($B_1C_3D_1$). For factor B (Halo implant dose), the level was varied from 2.83E13 atom/cm^{-3} to 2.87E13 atom/cm^{-3}, while the others were kept constant at the predicted optimal level ($A_3C_3D_1$). Next, factor C (S/D implant dose) level was varied from 2.25E18 atom/cm^{-3} to 2.29E18 atom/cm^{-3}, while the others were kept constant at the predicted optimal level ($A_3B_1D_1$). Lastly, factor D (S/D implant tilt angle) level was varied from 72º to 76º, while the others were fixed at the predicted optimal level ($A_3B_1C_3$). The simulation results for factor A, B, C and D upon GRG are depicted in Figure 9, 10, 11 and 12 respectively.

Based on the results, the optimal value of V_{TH} implant energy, halo implant dose, S/D implant dose and S/D implant tilt angle for the highest predicted GRG were observed at 28kev, 2.83E13 atom/cm^{-3}, 2.29E18 atom/cm^{-3} and 74º respectively. Therefore, these parameter values predicted by a well-trained ANN were re-simulated using Silvaco TCAD tools in order to verify the optimization results.

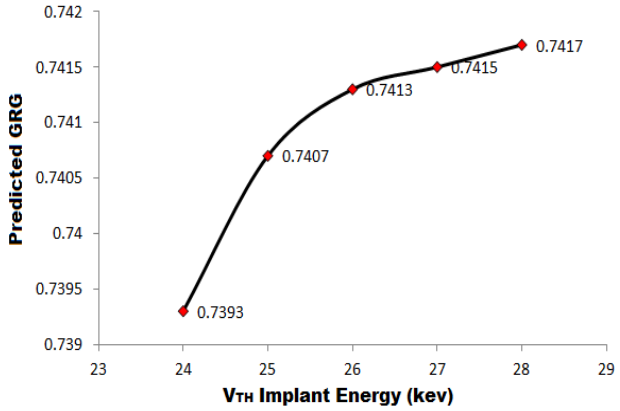

Figure 9: Simulation Results for Multiple Levels of V_{TH} Implant Energy

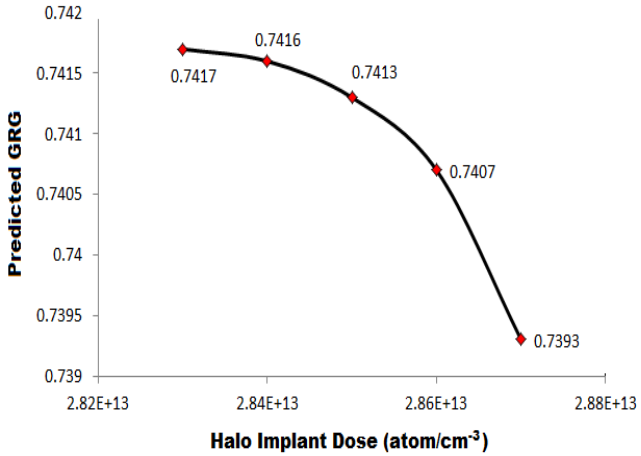

Figure 10: Simulation Results for Multiple Levels of Halo Implant Dose

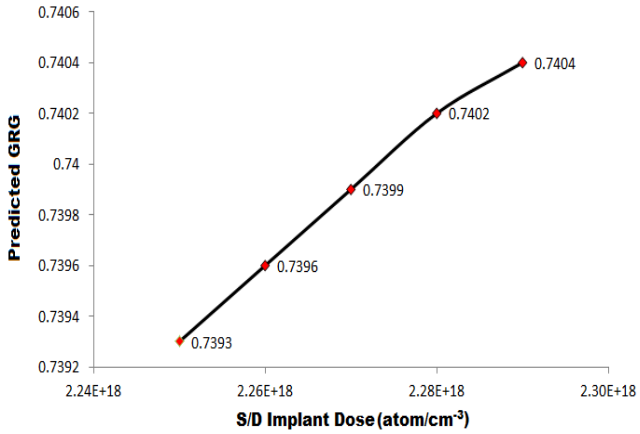

Figure 11: Simulation Results for Multiple Levels of S/D Implant Dose

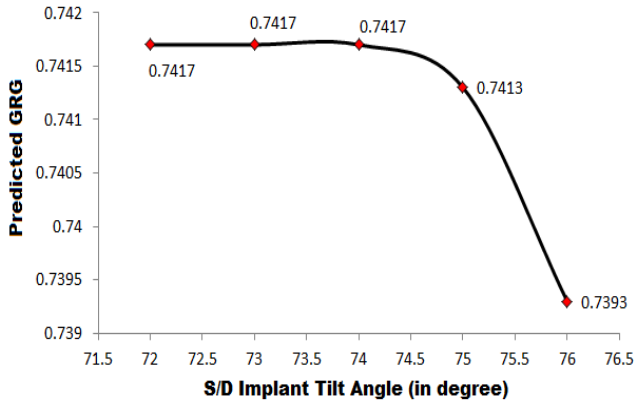

Figure 12: Simulation Results for Multiple Levels of S/D Implant Tilt Angle

V. VERIFICATION TEST

The verification test was performed to verify the optimal combination level of process parameters predicted by L_9 OA of Taguchi-based GRA with ANN with the actual results. The simulation based on the predicted process parameters via Taguchi-based GRA with ANN was conducted using Silvaco TCAD tools. The results showed that the predicted GRA was 0.7417. Table 9 shows the experimental results using the optimum process parameters predicted via by L_9 OA of Taguchi-based GRA and L_9 OA of Taguchi-based GRA with ANN.

Table 9
Results of Electrical Properties using L_9 OA of Taguchi-based GRA only and with ANN

Parameters& Electrical Properties	Optimization via L_9 OA of Taguchi-based GRA	Optimization via using L_9 OA of Taguchi-based GRA with ANN	ITRS 2013 Prediction [29]
V_{TH} Implant Energy (kev)	24	28	N/A
Halo Implant Dose (atom/cm^{-3})	2.87E13	2.83E13	N/A
S/D Implant Dose (atom/cm^{-3})	2.25E18	2.29E18	N/A
S/D Implant Tilt Angle (degree)	76	74	N/A
I_{ON} (µA/µm)	1599.3	1630.7	≥ 1480
I_{OFF} (A/µm)	8.655E-10	9.031E-10	≤ 100n
SS (mV/dec**)**	68.02	67.44	N/A
Predicted GRG via a well-trained ANN	0.7393	0.7417	N/A
Improvement in predicted GRG = 0.32 %			

The predicted GRG of process parameters via L_9 OA of Taguchi-based GRA with ANN owas slightly improved by 0.32%. The highest predicted GRG indicates the closeness of the I_{ON}, I_{OFF} and SS to their desired value. The I_{ON} value was improved by 1.92% after the optimization with a well-trained ANN. In fact, the I_{ON} was significantly increased by 9.24% compared to ITRS 2013 prediction. The I_{OFF} value was observed to be increased by 4.16% after the optimization with a well-trained ANN. However, the I_{OFF} value was still under 100 A/µm as predicted by ITRS 2013 [29]. The SS value after the optimization via L_9 OA of Taguchi-based GRA with ANN was slightly decreased by 0.85%.

Hence, it is concluded that the I_{ON}, I_{OFF} and SS of the device can be simultaneously optimized using a L_9 OA of Taguchi-based GRA with ANN. Moreover, the robust optimization can be executed through the assistance of a well-trained ANN, predicting the values outside the specified level of process parameters.

VI. CONCLUSION

In summary, multiple electrical properties of the TiO_2/WSi_x-based vertical double-gate MOSFET have been simultaneously optimized via L_9 OA of Taguchi-based GRA with a well-trained ANN. The multiple electrical properties such as I_{ON}, I_{OFF} and SS were converted into a single multi-performance characteristic, known as GRG. Four process parameters which were V_{TH} implant energy, halo implant dose, S/D implant dose and S/D implant tilt angle were selected as the inputs of a network, while the GRG was selected as an output of a network. Based on LMBP algorithm, a well trained ANN for GRG prediction was successfully developed with a R-value = 0.98087. The simulation via a well-trained ANN predicted that the 28kev of V_{TH} implant energy, 2.83E13 atom/cm^{-3} of halo implant dose, 2.29E18 atom/cm^{-3} of S/D implant dose and 74^o of S/D implant tilt angle produced the highest GRG. The most optimal value for I_{ON}, I_{OFF} and SS after the optimization were 1612.1 µA/µm, 8.801E-10 A/µm and 67.74 mV/dec respectively with 0.7417 of predicted GRG. It can be concluded that the implementation of a well-trained ANN has successfully assisted the L_9 OA of Taguchi-based GRA on finding the robust solution outside the specified level of process parameters. For future work, other device characteristics such as drain induced barrier lowering (DIBL), $I_{ON}/_{OFF}$ ratio and current density could be included in the optimization process which requires bigger sample size of DoE such as L_{27} and L_{36} orthogonal array.

ACKNOWLEDGMENT

The authors would like to thank to the Ministry of Higher Education (MOHE) of Malaysia, Mybrain15 and Centre for Telecommunication Research and Innovation (CeTRI), Faculty of Electronics and Computer Engineering (FKEKK), Universiti Teknikal Malaysia Melaka (UTeM) for sponsoring this research study.

REFERENCES

[1] Q. Xu *et al.*, "Ion-Implanted TiN Metal Gate With Dual Band-Edge Work Function and Excellent Reliability for Advanced CMOS Device Applications," *IEEE Trans. Electron Devices*, vol. 62, no. 12, pp. 4199–4205, 2015.

[2] R. Zhu *et al.*, "Cost-effective industrial n-type bifacial and IBC cells with ENERG i ™ P and B ion implantation," in *The 8th SNEC PV Power Expo*, 2014, pp. 1–6.

[3] R. B. Fair, "History of some early developments in ion-implantation technology leading to silicon transistor manufacturing," *Proc. IEEE*, vol. 86, no. 1, pp. 111–137, 1998.

[4] S. Saxena *et al.*, "Variation in Transistor Performance and Leakage in Nanometer-Scale Technologies," *IEEE Trans. Electron Devices*, vol. 55, no. 1, pp. 131–144, 2008.

[5] F. A. M. Rezali, S. F. W. M. Hatta, and N. Soin, "Scaling impact on design performance metric of sub-micron CMOS devices incorporated with halo," in *IEEE Regional Symposium on Micro and Nanoelectronics (RSM)*, 2015, pp. 1–4.

[6] B. C. Paul, S. Fujita, M. Okajima, T. H. Lee, H. S. P. Wong, and Y. Nishi, "Impact of a process variation on nanowire and nanotube device performance," *IEEE Trans. Electron Devices*, vol. 54, no. 9, pp. 2369–2376, 2007.

[7] C. Y. Chen, J. T. Lin, and M. H. Chiang, "Comparative study of process variations in junctionless and conventional double-gate MOSFETs," in *IEEE Nanotechnology Materials and Devices Conference, IEEE NMDC 2013*, 2013, pp. 1–2.

[8] H. Ramakrishnan, "Variability: Analysis and Impact on Circuit Response," 2009.

[9] V. Sukhdeve and S. K. Ganguly, "Utility of Taguchi Based Grey Relational Analysis to optimize any Process or System," *Int. J. Adv. Eng. Res. Stud.*, vol. Jan-March, pp. 242–250, 2015.

[10] F. Salehuddin, I. Ahmad, F. A. Hamid, and A. Zaharim, "Application of Taguchi Method in Optimization of Gate Oxide and Silicide Thickness for 45nm NMOS Device," *Int. J. Eng. Technol.*, vol. 9, no. 10, pp. 94–98, 2009.

[11] F. Salehuddin *et al.*, "Analysis of Threshold Voltage Variance in 45nm N-Channel Device Using L_{27} Orthogonal Array Method," *Adv. Mater. Res.*, vol. 903, pp. 297–302, Feb. 2014.

[12] A. H. Afifah Maheran, P. S. Menon, I. Ahmad, and S. Shaari, "Optimisation of Process Parameters for Lower Leakage Current in 22 nm n-type MOSFET Device using Taguchi Method," *J. Teknol.*, vol. 68, no. 4, pp. 1–5, 2014.

[13] A. H. Afifah Maheran, I. Ahmad, S. Shaari, and H. A. Elgomati, "22nm NMOS device with lowest leakage current , optimized using Taguchi Method," *Commun. Circuits Educ. Technol.*, pp. 170–173, 2014.

[14] S. Te Lin *et al.*, "Application of grey-relational analysis to find the most suitable watermarking scheme," *Int. J. Innov. Comput. Inf. Control*, vol. 7, no. 9, pp. 5389–5401, 2011.

[15] N. Aggarwal and S. K. Sharmar, "Optimization of process parameters by Taguchi based Grey Relational Analysis :," *Int. J. Curr. Eng. Technol.*, vol. 4, no. 4, pp. 2792–2796, 2014.

[16] M. A. Wahid, B. O. P. Soepangkat, and B. Pramujati, "Multi Response Optimization in Face Milling Process of ASSAB XW-42 Tool Steel with Liquid Nitrogen Cooling using Taguchi-Grey-Fuzzy Method," *ARPN J. Eng. Appl. Sci.*, vol. 11, no. 4, pp. 2711–2717, 2016.

[17] H. Hasani, S. A. Tabatabaei, and G. Amiri, "Grey Relational Analysis to Determine the Optimum Process Parameters for Open-End Spinning Yarns," *J. Eng. Fiber. Fabr.*, vol. 7, no. 2, pp. 81–86, 2012.

[18] H. L. Lin, "The use of the Taguchi method with grey relational analysis and a neural network to optimize a novel GMA welding process," *J. Intell. Manuf.*, vol. 23, pp. 1671–1680, 2012.

[19] I. S. Kim, Y. J. Jeong, and C. W. Lee, "Prediction of Welding Parameters for Pipeline Welding using an Intelligent System," *Intenational J. Adv. Manuf. Technol.*, vol. 22, pp. 713–719, 2003.

[20] C. T. Soo and T. L. Chiang, "Optimizing the IC Wire Bonding Process using a Neural Network/Genetic Algorithm Approach," *J. Intell. Manuf.*, vol. 14, pp. 229–238, 2003.

[21] K. R. Kenghe and P. M. Patare, "Optimization of Tribological Properties Using Grey Relational Analysis and Artificial Neural Network," *Int. Eng. Res. J.*, vol. 1, no. 1, pp. 1022–1028, 2015.

[22] A. K. Yadav, H. Malik, and A. P. Mital, "Artificial Neural Network Fitting Tool Based Prediction of Solar Radiation for Identifying Solar Power Potential," *J. Electr. Eng.*, pp. 1–5, 2015.

[23] K. E. Kaharudin, F. Salehuddin, A. S. M. Zain, and M. N. I. A. Aziz, "Taguchi Modeling With The Interaction Test For Higher Drive Current in WSIx/TIO2 Channel Vertical Double Gate NMOS Device," *J. Theor. Appl. Inf. Technol.*, vol. 90, no. 1, pp. 185–193, 2016.

[24] K. E. Kaharudin *et al.*, "Multi-response optimization in vertical double gate PMOS device using Taguchi method and grey relational analysis," in *IEEE International Conference on Semiconductor Electronics (ICSE)*, 2016, pp. 64–68.

[25] V. K. Yadav and A. K. Rana, "Impact of Channel Doping on DG-MOSFET Parameters in Nano Regime-TCAD Simulation," *Int. J. Comput. Appl.*, vol. 37, no. 11, pp. 36–41, 2012.

[26] S. Xiong and J. Bokor, "Sensitivity of Double-Gate and FinFET Devices to Process Variations," *IEEE Trans. Electron Devices*, vol. 50,

no. 11, pp. 2255–2261, 2003.
[27] A. a. Orouji and M. J. Kumar, "Nanoscale SOI MOSFETs with electrically induced source/drain extension: Novel attributes and design considerations for suppressed short-channel effects," *Superlattices Microstruct.*, vol. 39, pp. 395–405, 2006.
[28] V. C. Sekhar, S. A. Hussain, V. Pandurangadu, and T. S. Rao, "Grey Relational Analysis to Determine Optimum Process Parameters of „ Emu " Feather Fiber Reinforced Epoxy Composites," *Int. J. Emerg. Technol. Adv. Eng.*, vol. 5, no. 8, pp. 86–90, 2015.
[29] ITRS, "International Technology Roadmap Semiconductor," 2013.